Hindawi
Shock and Vibration
Volume 2018, Article ID 8269384, 16 pages
https://doi.org/10.1155/2018/8269384

Research Article

Effects of Surface Waviness on the Nonlinear Vibration of Gas Lubricated Bearing-Rotor System

Jian Li,[1,2] Shaoqi Yang,[1,3] Xiaoming Li,[1,3] and Qing Li [1,2,3]

[1]*State Key Laboratory of Technologies in Space Cryogenic Propellants, Beijing 100190, China*
[2]*School of Energy Power and Engineering, Huazhong University of Science and Technology, Wuhan, Hubei 430074, China*
[3]*University of Chinese Academy of Sciences, Beijing 100049, China*

Correspondence should be addressed to Qing Li; simple_lxcy2014@163.com

Received 30 May 2018; Accepted 25 September 2018; Published 4 November 2018

Academic Editor: Konstantin Avramov

This paper presents the effects of the surface waviness on the nonlinear dynamic performance of a gas bearing-rotor system. The coupled vibration with the elastomer is taken into consideration to fit the actual engineering application. The effects of the directions, the amplitudes, and the numbers of waves to the nonlinear dynamic performance are investigated. The results show that the existence of the surface waviness in the circumferential direction can improve the stability of the system obviously. But the surface waviness in the axial direction is damage to the system. The nonlinear dynamic performance of the system is insensitive to the number of surface waviness. The increase of the amplitude of the waviness in circumferential direction can improve the stability of the system.

1. Introduction

Bearing is an essential component of most rotating machines. They provide the load capacity and stiffness to support shafts against static loads and dynamic forces. Gas lubricating journal bearings have many advantages of less heat generation, more environment friendly, higher accuracy, and longer lives by comparing with traditional oil bearings. Thus, the gas lubricating bearing-rotor system is widely used in engineering applications such as turboexpanders in large-scale cryogenic systems, superprecision machine tools, and high-speed machines [1, 2]. However, the inherent characteristic of compressibility and low viscidity of gas may cause instability to the gas bearing-rotor system which limits the range of the application of gas bearings. Furthermore, the low viscosity of gas makes a thin gas film generally lower than 50 micrometers. As the result, the assumption of the journal bearing is that the smooth surface is far from bearing practical application especially for bearing-rotor system operating under a relatively small film thickness [3].

Manufacturing error may cause some waves on the surfaces of bearing. These waves can change the thickness distribution of the gas film which can significantly influence the static and dynamic performance of the gas bearing-rotor system. During the past years, authors have published many articles about the effects of the surface waviness on the performance of the bearing. Dimofte [4] compared the three-waved journal bearing with both the three-wave-groove bearing and three-lobe bearing [5], they concluded that the load capacity of the wave bearing is better than other types, and the performance of the wave bearing is dependent on the parameters and position of waves. Rasheed [3] studied the influence of circumferential, axial, and combined surface waviness on the performance of plain cylindrical bearings. They noted that the circumferential waviness can increase the load capacity and decrease the friction variable when the wave number is below 9, and the axial waviness has the adverse effects on load capacity and friction. Kwan and Post [6] studied the influence of manufacturing error of rectangular thrust bearing on the static load and stiffness performance. They concluded that the load capacity and stiffness are sensitive to the manufacturing errors. Nagaraju

et al. [7] studied the combined influence of bearing flexibility and surface roughness on the characteristics of the journal bearing system. The results indicated that the longitudinal roughness pattern of the bearing can improve the load capacity. Ene et al. [8] used both the transient and small perturbation methods to investigate the dynamic behavior of three-wave journal bearing system. The results showed the influence of the wave amplitude and oil supply pressure on the threshold of stability. Sharma and Kushare [9] investigated the influence of surface roughness on the performance of two-lobe journal bearing. The results indicated that the performance of the bearing system is significantly affected by the orientation of roughness. And thus, the performance of bearing can be enhanced by the proper selection of the roughness pattern parameter. Wang et al. [10] studied the influence of the waves of bearing surface on the static and dynamic performance of the aerostatic journal bearing. The results showed that the wave amplitudes significantly affect the static and dynamic performance of the bearing.

The stability is the most important character for the bearing-rotor system. Large number of articles has been published to investigate the stability of gas-lubricant bearing-rotor system. Among these papers, two different approaches were published to analyze the dynamic stability of the rotor-bearing system: one is the linear small perturbation analysis and another is the nonlinear transient analysis.

Linear small perturbation theory assumes that the journal obit whirls around its equilibrium position with a small perturbation. This assumption makes the dynamic stiffness, and dynamic damping coefficients can be computed. And then, the whirl frequency and critical mass can be computed by these dynamic coefficients. This method can provide the instability boundary. Thus, the stability of the system can be estimated by the threshold. However, this method cannot present the characters of the motion.

Gross and Zachmanoglou [11] studied the performance of the self-acting journal bearing with infinite length by using the small perturbation method. The calculation results are valid for other types of bearings with high accuracy. Belforte et al. [12] investigated dynamic coefficients of self-acting gas bearing, they used the developed mathematical model, and the results were in good agreement with the results using the nonlinear distribution parameter model. Yang et al. [13] studied the dynamic coefficients of self-acting tilting pad gas bearing, and the results showed the relationship between dynamic coefficients and tilting pad perturbation. Yu et al. [14] used numerical simulations and experiments to investigate the influence of perturbations on the dynamic stiffness for aerostatic bearings. The results revealed that the dynamic stiffness coefficients are more sensitive to the frequency of perturbation than the amplitude; thus, they concluded that the dynamic stiffness can be enhanced through active control which can generate perturbations.

In nonlinear transient analysis, the time-dependent Reynolds equation is solved to get the transient forces, and then, the transient journal center obits are obtained by solving the motion equations. The stability of the system can be judged by the shape of obits. The nonlinear dynamic characters are available by using this method which is different from the perturbation analysis.

Kim and Noah [15] coupled harmonic balance with alternating frequency technique to obtain synchronous and subsynchronous whirling motions of a Jeffcott rotor-bearing system. The results showed that as the parameters of the system changed the boundary of flip bifurcation were obtained. Wang et al. [16–20] investigated the bifurcation performance of rigid rotor and flexible rotor supported by a pair of gas bearing, and the results presented a better understanding to the nonlinear dynamic characters of the gas bearing-rotor system. From the calculation results, we can also find that the dynamic behavior of the rotor center is very complex which includes periodic and subharmonic response. Rashidi et al. [1, 2] presented the effect of operating parameters on nonlinear dynamic performance for noncircular journal gas-lubricated bearing-rotor system. The complex nonlinear dynamic behaviors such as periodic, KT-periodic, and quasiperiodic responses were analyzed by using dynamic trajectory, the Poincare maps, and bifurcation diagrams. Hassini and Arghir [21] used the dynamic coefficients to analyze the nonlinear characteristics, and the results were in good agreement with the results calculated by nonlinear transient Reynolds equations. Abbasi et al. [22] studied the vibration control of the rotating machine with a high-static low-dynamic stiffness suspension. In their study, the complex nonlinear dynamic behavior was showed, and the results present that the method can suppress the nonperiodic behavior in the considered speed range.

Generally speaking, the vibrations of most manufacture machines are inevitable which will cause the surface to be unsmooth. The effects of waves on static performances and dynamic coefficients of bearing are investigated in most previous published articles. However, few papers have mentioned the effects of waves on the stability and nonlinear dynamic performance of the gas bearing. Thus, in this paper, the effects of surface waviness in circumferential and axial directions on the nonlinear dynamic characteristics of the rotor-gas bearing system have been investigated. The method used in this paper is nonlinear transient approach which is similar to the previous articles [18, 23], but our focuses are different. In practical engineering, the elastomers are mounted between bearing and shaft; thus, the elastomer suspension is taken into consideration. The results in this paper can provide guidance on the design and manufacture of the gas bearing system.

2. Numerical Solution of Gas Pressure Distribution

The model in this paper is a massless shaft with a disk supported by a pair of self-acting gas journal bearings. Generally speaking, the manufacture precision of rotors is always better than that of bearings, so, the waves on the surface of rotors can be neglected [22]. In this paper, the journal bearings used for calculation include axial and

circumferential surface waviness which is shown in Figure 1. Before numerical simulation, some design assumptions are given as follows [16–18, 23]:

(1) Isothermal flow: due to the heat conductivity ability of the bearing material (copper) is much bigger than that of gas, the heat generation in the gas film will conduct away quickly. Thus, the temperature of gas is constant.

(2) Curvature insensitive: the gas film thickness is much smaller than the diameter of the shaft. So, the change of velocity caused by the curvature is neglected.

(3) Constant viscosity: due to the viscosity of gas is insensitive to the changes of pressure, we assume it as a virtually constant.

(4) The side flow of the bearing can be neglected.

To simplify the model of surface waves, we assume that the form of waves fits the function of sinusoidal; thus, the waviness in circumferential direction can be described as the following form [10, 24]:

$$\delta = A\sin\left(\frac{2\pi R}{\lambda}\theta\right). \tag{1}$$

The waves in axial direction of the bearing can be denoted as

$$\delta = A\sin\left(\frac{2\pi}{\lambda}y\right). \tag{2}$$

Based on the assumption above, the pressure distribution of the gas film can be described by the Reynolds equation:

$$\frac{\partial}{\partial x}\left(\frac{ph^3}{\mu}\frac{\partial p}{\partial x}\right) + \frac{\partial}{\partial y}\left(\frac{ph^3}{\mu}\frac{\partial p}{\partial y}\right) = 6\left[U\frac{\partial}{\partial x}(ph) + 2\frac{\partial}{\partial t}(ph)\right], \tag{3}$$

where h is the gas film thickness and can be denoted as

$$h = Cr(1 + \varepsilon\cos\varphi) - \delta. \tag{4}$$

Some dimensionless parameters are defined as follows to transform Equation (3) into polar coordinate and nondimensionalized:

$$\begin{aligned} P &= \frac{p}{P_a}, \\ U &= R\varpi, \\ \tau &= \varpi t, \\ \Lambda &= \frac{6\mu\varpi}{P_a}\left(\frac{R}{Cr}\right)^2, \\ H &= \frac{h}{Cr}, \\ \theta &= \frac{x}{R}, \\ \eta &= \frac{y}{R}. \end{aligned} \tag{5}$$

Taking the dimensionless parameters above into Equation (3), the dimensionless Reynolds equation is obtained and can be written as

$$\frac{\partial}{\partial\theta}\left(PH^3\frac{\partial P}{\partial\theta}\right) + \frac{\partial}{\partial\eta}\left(PH^3\frac{\partial P}{\partial\eta}\right) = \Lambda\frac{\partial}{\partial\theta}(ph) + 2\Lambda\frac{\partial}{\partial\tau}(ph). \tag{6}$$

The finite difference method is used to get the pressure distribution of the gas film. The discretized scheme of the Reynolds equation was derived by using the central difference method in circumferential and axial directions and the implicit backwards method in time τ. The methods used in this paper are similar to the previous articles [18, 23], and the discretized version can be described as

$$\begin{aligned} &\frac{3\left(H_i^{n+1}\right)^2}{2}\frac{\left(H_{i+1}^{n+1} - H_{i-1}^{n+1}\right)}{2\Delta\theta}\frac{\left(S_{i+1,j}^{n+1} - S_{i-1,j}^{n+1}\right)}{2\Delta\theta} + \left(H_{i,j}^{n+1}\right)^3\left(\frac{S_{i+1,j}^{n+1} - 2S_{i,j}^{n+1} + S_{i-1,j}^{n+1}}{(\Delta\theta)^2}\right) + \frac{\left(H_i^{n+1}\right)^3}{2}\frac{\left(S_{i,j+1}^{n+1} - 2S_{i,j}^{n+1} + S_{i,j-1}^{n+1}\right)}{(\Delta\eta)^2} \\ &= \Lambda P_{i,j}^{n+1}\left(\frac{H_{i+1}^{n+1} - H_{i-1}^{n+1}}{2\Delta\theta}\right) + \Lambda H_i^{n+1}\left(\frac{P_{i+1,j}^{n+1} - P_{i-1,j}^{n+1}}{2\Delta\theta}\right) + 2\Lambda H_i^{n+1}\left(\frac{P_{i,j}^{n+1} - P_{i,j}^{n}}{\Delta\tau}\right) + 2\Lambda P_{i,j}^{n+1}\left(\frac{H_{i,j}^{n+1} - H_{i,j}^{n}}{2\Delta\tau}\right), \end{aligned} \tag{7}$$

where $S = P^2$; $i = 1, 2, \ldots, N$; $j = 1, 2, \ldots, M$.

The film thickness distribution is depended by the position of the rotor. For parameter $P_{i,j}^{n+1}$, the equation is a quadratic equation with one unknown and determined by the pressure of the surrounding four nodes $(i-1, j)$, $(i+1, j)$, $(i, j+1)$, and $(i, j-1)$.

The pressure distribution of the gas film between the rotor and bearing enables the estimation of the supporting force which is acting on the rotor. The supporting force can be described as

$$\begin{aligned} f_{gx} &= P_a R^2\int_{-(L/R)}^{L/R}\int_0^{2\pi} P(\theta,\eta)\cos\theta\, d\theta\, d\eta, \\ f_{gy} &= P_a R^2\int_{-(L/R)}^{L/R}\int_0^{2\pi} P(\theta,\eta)\sin\theta\, d\theta\, d\eta, \end{aligned} \tag{8}$$

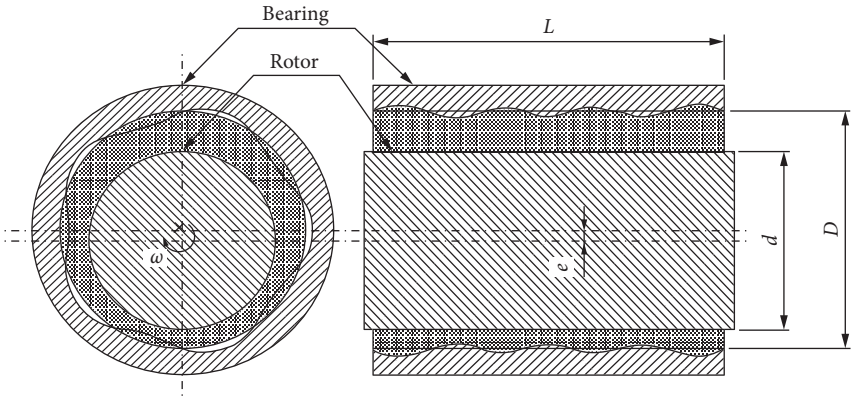

Figure 1: Model of self-acting gas journal bearing with surface waviness.

where $P(\theta, \eta)$ is the pressure distribution in the dimensionless coordinate system.

3. Rotor Dynamic Equations and Obits Calculation Procedure

In this paper, we use the nonlinear transient approach to investigate the stability of the rotor-bearing system. The model for calculation is a massless rotor with a disk, and it was supported by a pair of self-acting gas bearings. In engineering reality, the elastic dampers such as O-rings are mounted between bearings and shell to improve its stability, shown in Figure 2. The damping force of the elastomer obeys the viscous damping law which is one of the simplest and most widely used. This model is expressed as [25–27]

$$f_{\mathrm{d}} = \mathrm{sign}\left(\dot{x}_{\mathrm{b}}\right) c \left|\dot{x}_{\mathrm{b}}\right|^{\gamma}, \tag{9}$$

where γ is the damping exponent; sign() is the signum function. The case $\gamma = 1$ is chose which indicates the linear viscous damping model and used for calculation.

Thus, the equation of motion of the rotor and bearing in transient state can be written as

$$\begin{aligned}
m_{\mathrm{s}} \frac{d^2 x_{\mathrm{s}}}{dt^2} &= f_{\mathrm{ex}} - f_{\mathrm{gx}} + m_{\mathrm{s}} e_{\mathrm{ub}} \overline{w}^2 \sin(\overline{w}t), \\
m_{\mathrm{s}} \frac{d^2 y_{\mathrm{r}}}{dt^2} &= f_{\mathrm{ey}} - f_{\mathrm{gy}} + m_{\mathrm{s}} e_{\mathrm{ub}} \overline{w}^2 \cos(\overline{w}t), \\
m_{\mathrm{b}} \frac{d^2 x_{\mathrm{b}}}{dt^2} &= f_{\mathrm{gx}} - k x_{\mathrm{b}} - \mathrm{sign}\left(\dot{x}_{\mathrm{b}}\right) c \left|\dot{x}_{\mathrm{b}}\right|^{\gamma}, \\
m_{\mathrm{b}} \frac{d^2 y_b}{dt^2} &= f_{\mathrm{gy}} - k y_{\mathrm{b}} - \mathrm{sign}\left(\dot{y}_{\mathrm{b}}\right) c \left|\dot{y}_{\mathrm{b}}\right|^{\gamma}.
\end{aligned} \tag{10}$$

The nondimensional groups can be defined as follows:

$$\begin{aligned}
X_{\mathrm{s}} &= \frac{x_{\mathrm{s}}}{Cr}, \\
Y_{\mathrm{s}} &= \frac{y_{\mathrm{s}}}{Cr}, \\
X_{\mathrm{b}} &= \frac{x_{\mathrm{b}}}{Cr}, \\
Y_{\mathrm{b}} &= \frac{y_b}{Cr}, \\
F_{\mathrm{ex}} &= \frac{f_{\mathrm{ex}}}{P_{\mathrm{a}} RL}, \\
F_{\mathrm{ey}} &= \frac{f_{\mathrm{ey}}}{P_{\mathrm{a}} RL}, \\
F_{\mathrm{gx}} &= \frac{f_{\mathrm{gx}}}{P_{\mathrm{a}} RL}, \\
F_{\mathrm{gy}} &= \frac{f_{\mathrm{gy}}}{P_{\mathrm{a}} RL}, \\
M_{\mathrm{s}} &= \frac{m_{\mathrm{s}} Cr \overline{w}^2}{P_{\mathrm{a}} RL}, \\
M_{\mathrm{b}} &= \frac{m_{\mathrm{b}} Cr \overline{w}^2}{P_{\mathrm{a}} RL}, \\
\rho &= \frac{e_{\mathrm{ub}}}{Cr}, \\
K &= \frac{kCr}{P_{\mathrm{a}} RL}, \\
C &= \frac{c(Cr\overline{w})^{\gamma}}{P_{\mathrm{a}} RL}.
\end{aligned} \tag{11}$$

Substituting Equation (11) into Equation (10), we will get the dimensionless dynamic equations as follows:

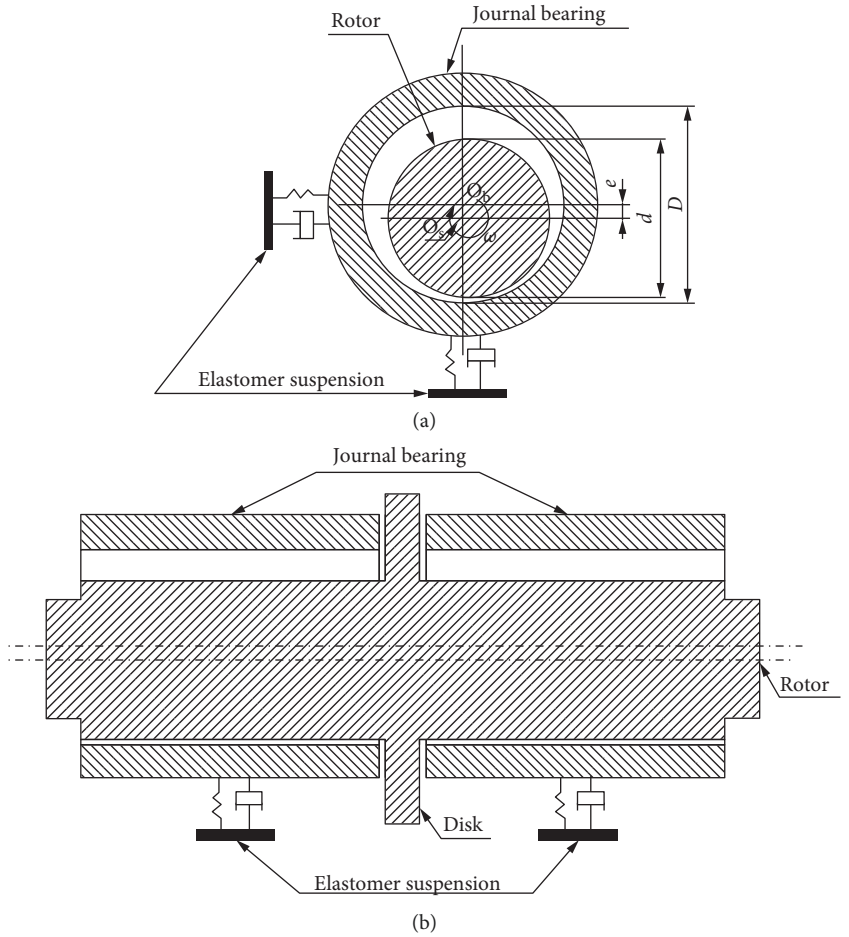

Figure 2: Schematic of a rigid rotor (massless shaft and disk) in journal bearing with elastic damper.

$$\frac{d^2X_s}{d\tau^2} = \frac{F_{ex} - F_{gx} + M_s\rho\sin(\tau)}{M_s} = A_{sx},$$

$$\frac{d^2Y_s}{d\tau^2} = \frac{Y_{ex} - Y_{gx} + M_s\rho\cos(\tau)}{M_s} = A_{sy},$$

$$\frac{d^2X_b}{d\tau^2} = \frac{F_{gx} - KX_b - \text{sign}(\dot{X})C\left|\dot{X}_b\right|^\gamma}{M_b} = A_{bx}, \quad (12)$$

$$\frac{d^2Y_b}{d\tau^2} = \frac{Y_{gx} - KY_b - \text{sign}(\dot{Y})C\left|\dot{Y}_b\right|^\gamma}{M_b} = A_{by}.$$

As we get acceleration of the rotor and bearing in horizontal and vertical directions, the center obits of rotor and bearing can be acceptable by using the following equation:

$$V_{sx} = V_{sx0} + A_{sx}\Delta\tau,$$

$$V_{sy} = V_{sy0} + A_{sy}\Delta\tau,$$

$$V_{bx} = V_{bx0} + A_{bx}\Delta\tau,$$

$$V_{by} = V_{by0} + A_{by}\Delta\tau,$$

$$X_s = X_{s0} + V_{sx}\Delta\tau + \frac{1}{2}A_{sx}\Delta\tau^2, Y_s = Y_{s0} + V_{sy}\Delta\tau + \frac{1}{2}A_{sy}\Delta\tau^2, X_b = X_{b0} + V_{bx}\Delta\tau + \frac{1}{2}A_{bx}\Delta\tau^2, Y_b = Y_{b0} + V_{by}\Delta\tau + \frac{1}{2}A_{by}\Delta\tau^2. \quad (13)$$

Computation of the center trajectory of rotor and bearing is an iterative procedure. The procedure begins with the initial equilibrium state. The initial position of the rotor (X_0, Y_0) is a static balance position which is defined by the external loading and rotational speed. To estimate the influence of the initial condition, the first 600 periodic calculation data can be ignored and the nonlinear behavior analysis is based on the data after the vibration is stable. The initial velocities of the rotor in two different directions are assumed to be zero.

4. Results and Discussion

In order to verify the correctness of the program, the attitude angle φ and supporting force F of a self-acting journal gas bearing with smooth surface are calculated and compared

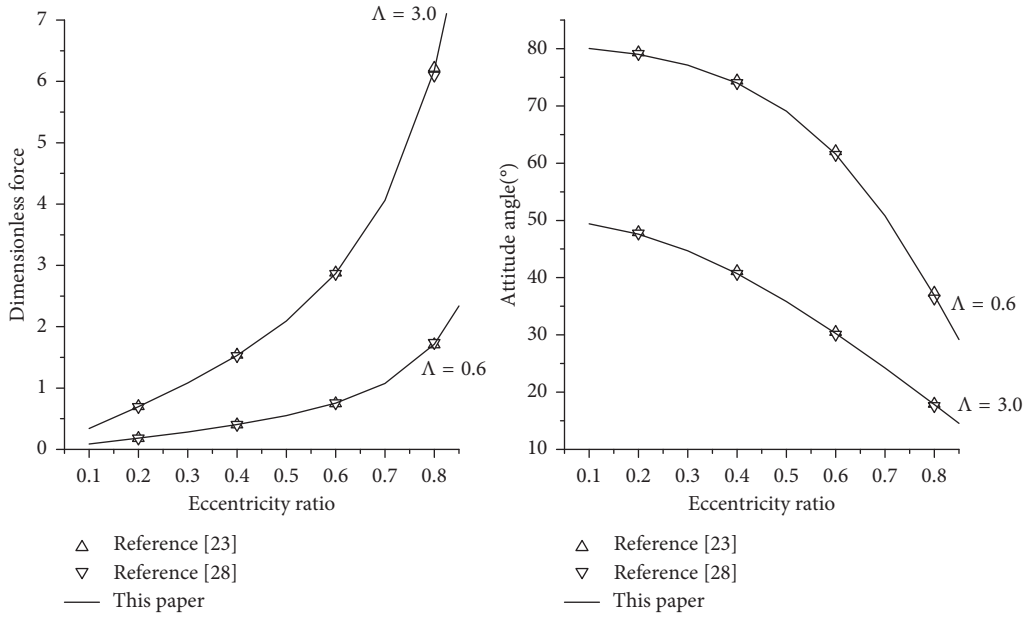

Figure 3: Comparison of steady state calculation results for journal gas bearing, $D = L$.

with previous investigations [23, 28], as is shown in Figure 3. The results in this paper are in good agreement with the previous investigations; thus, the validity of the program is verified.

The rotor unbalance mass is an important parameter for rotating machine which influence the response of the rotor-bearing system [28, 29]. In this paper, what we focused on is the influence of the surface waviness to the nonlinear dynamic response. So, the single rotor unbalance value (0.15 μm) is selected in this study. The rotor-bearing system is used in the turbomachine with a superhigh speed. Thus, the mass of the rotor is usually quite small, less than 0.5 kg.

In the numerical integration, the aspect ratio (L/D) of self-acting journal gas bearing for calculation is chosen as 1.44. The lubricant in the film is air. The parameters of elastomer are set as follows: $k = 4e6$N/m, $\xi = 0.005$, and $\gamma = 1$. To show the influence of the surface waviness to the nonlinear dynamic response clearly, the bifurcation diagrams of the rotor-bearing system with flat surface are plotted, which is presented in Figure 4. From the results, we can conclude that when the half mass of the rotor is equal or less than 0.18 kg, the rotor center presents a regular periodic motion. But, motion loses its regularity and becomes irregular when the half mass of the rotor increased to 0.19 kg.

Figure 5 shows the bifurcation diagrams of the rotating system with circumferential surface waviness. In this calculation, we assume that the surface waviness is only included in the circumferential direction of the bearing, and the number of waves is equal to 5, and the amplitude of the waves is 1 micrometer. Compared with the results in Figure 4, the discrete point of the system with circumferential waviness is much bigger than the system with flat surface which indicated that the waviness in circumferential direction can increase the stability of the system obviously.

In order to show nonlinear dynamic performance of the system clearly, a set of maps such as the rotor center obits, phase portraits, logarithmic spectra maps in two directions, and Poincare maps are used to analyze the nonlinear dynamic performance in different conditions.

Figures 6(a)–13(a) are the obits of the rotor center in the (X, Y) plane; Figures 6(b)–13(b) and 6(c)–13(c) are phase portraits in $(X, \dot{X})$ and $(Y, \dot{Y})$ planes, respectively; Figures 6(d)–13(d) and 6(e)–13(e) are the logarithmic spectra of the nondimensional displacement in horizontal and vertical, respectively; Figures 6(f)–13(f) are Poincare maps in the (X, Y) plane.

From Figures 6–8, when the half mass of the rotor is less than 0.75 kg, the vibration is mainly caused by the mass unbalance, the frequency of rotating is much bigger than subharmonic frequency; thus, the rotor center obits show a regular periodic motion. When the half mass of the rotor is in the range of 0.75 kg and 1 kg, the amplitude of subharmonic vibration increased and cannot be ignored. The motion losses its periodic motion, and subharmonic periodic motion appears. However, the amplitude of motion is also small. When the half mass of the rotor is bigger than 1.0 kg, shown in Figures 8 and 9, the amplitude of vibration becomes much bigger and a closed curve occurs in the Poincare map, which indicated that quasiperiodic motion appears.

The effects of the number of waviness in the circumferential direction on the nonlinear dynamic performance of the system are analyzed in which different numbers of waviness ($N = 3, 5,$ and 7) with $m_s = 1.0$ kg, $\xi = 0.005$, $k = 4e6N/m$ are used for calculation. Figures 8–11 show the obits, logarithmic spectrum maps, and Poincare map with surface waviness ($N = 3, 5,$ and 7), respectively. The comparison between different numbers of waviness in circumferential direction shows that the number of waviness do not change the nonlinear dynamic performance of the system, but the amplitude of the vibration declines slightly with the increase of the number of waviness (shown in the

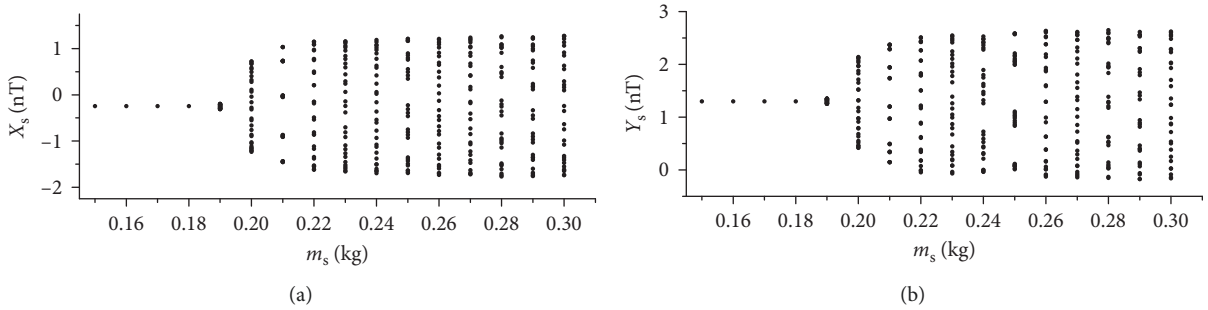

Figure 4: Bifurcation diagrams of rotor: (a)X_s (nT) and (b)Y_s (nT) versus half mass of rotor.

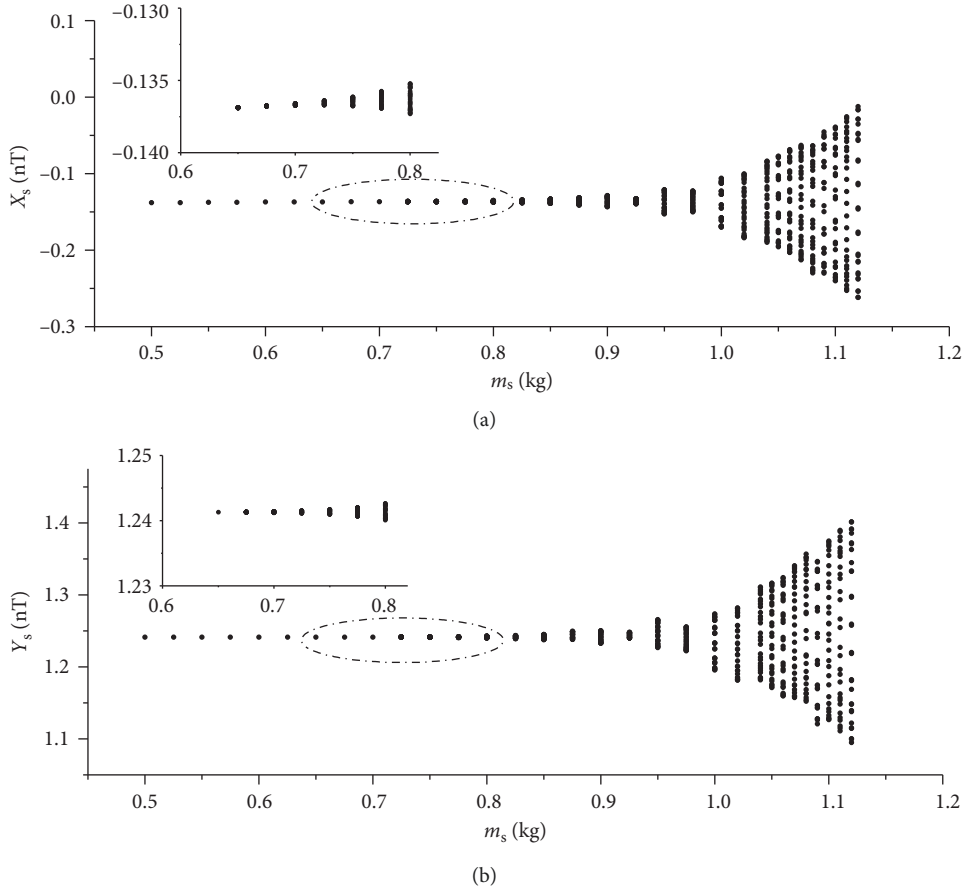

Figure 5: Bifurcation diagrams of rotor center with circumferential surface waviness: (a) X_s (nT) and (b) Y_s (nT) versus half mass of rotor.

logarithmic spectrum maps). The increase of the number of waves can only improve the static and dynamic performance of the bearing slightly which is not enough to change the nonlinear dynamic behavior of the system.

Figures 8, 12, and 13 display the obits, logarithm amplitude spectrum maps, and Poincare maps of the rotor center with different surface waviness amplitudes in circumferential direction. In this solution, three cases (A = 1, 2, and 3) with other parameters such as m_s = 1 kg, ξ = 0.005, and k = 4e6N/m are used and compared. The nonlinear dynamic performance changes from quasiperiodic motion (A = 1) to regular periodic motion (A = 4). This means the large amplitude of the waviness can increase the stability of the system, but the amplitude of the waviness is restricted by the gas clearance. From the obits and logarithm spectrum maps in these pictures above, we can find that the increase of the amplitude of the surface waviness in circumferential direction can decline the amplitude of the subharmonic frequency. That is because the increase of the amplitude of the waviness can increase the static and dynamic performance.

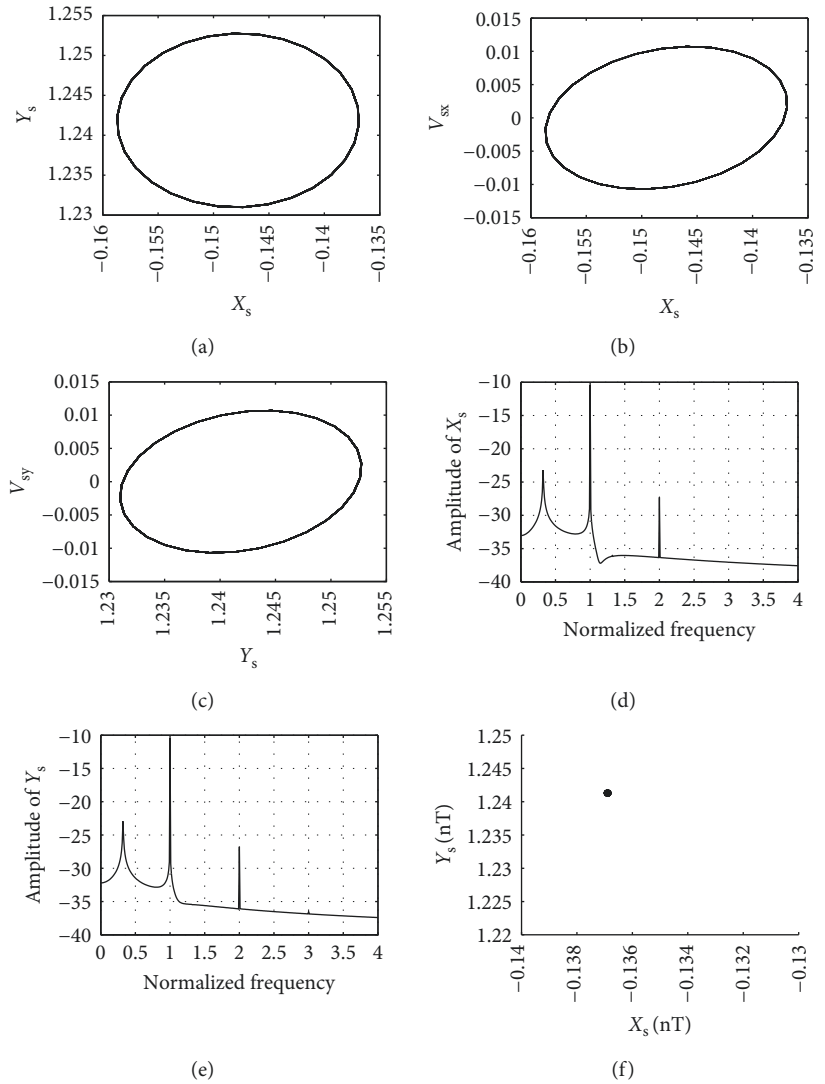

Figure 6: Obits, Poincare map, and amplitude spectrum of rotor center (m_s = 0.65 kg, ξ = 0.005, k = 4e6N/m, A = 1μm, and N = 5).

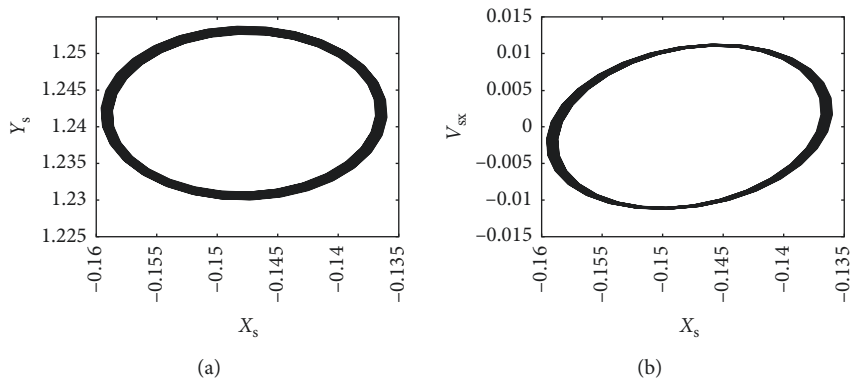

Figure 7: Continued.

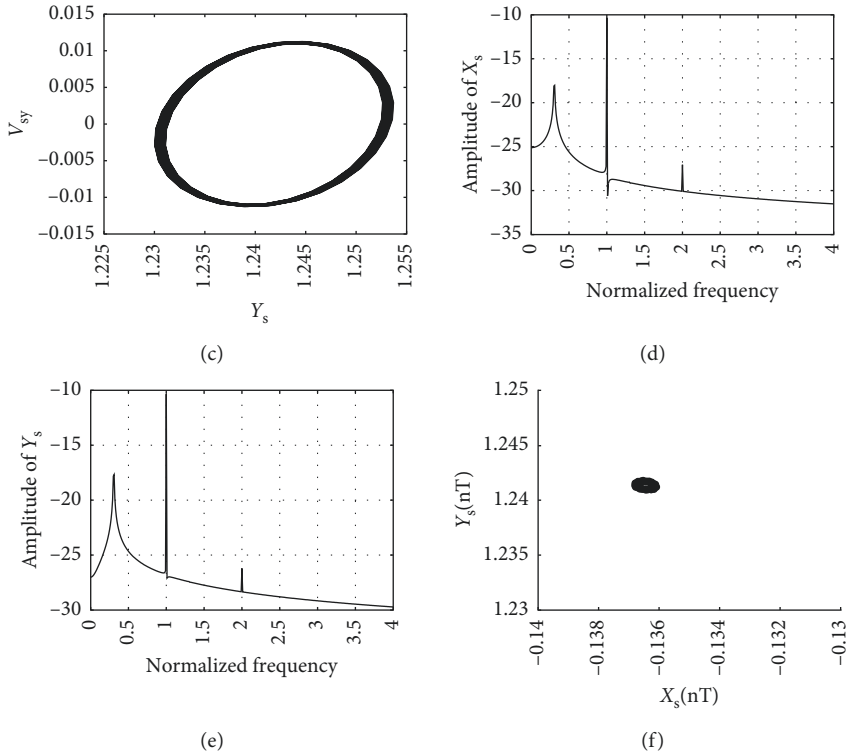

Figure 7: Obits, Poincare map, and amplitude spectrum of rotor center (m_s = 0.75 kg, ξ = 0.005, k = 4e6N/m, A = 1μm, and N = 5).

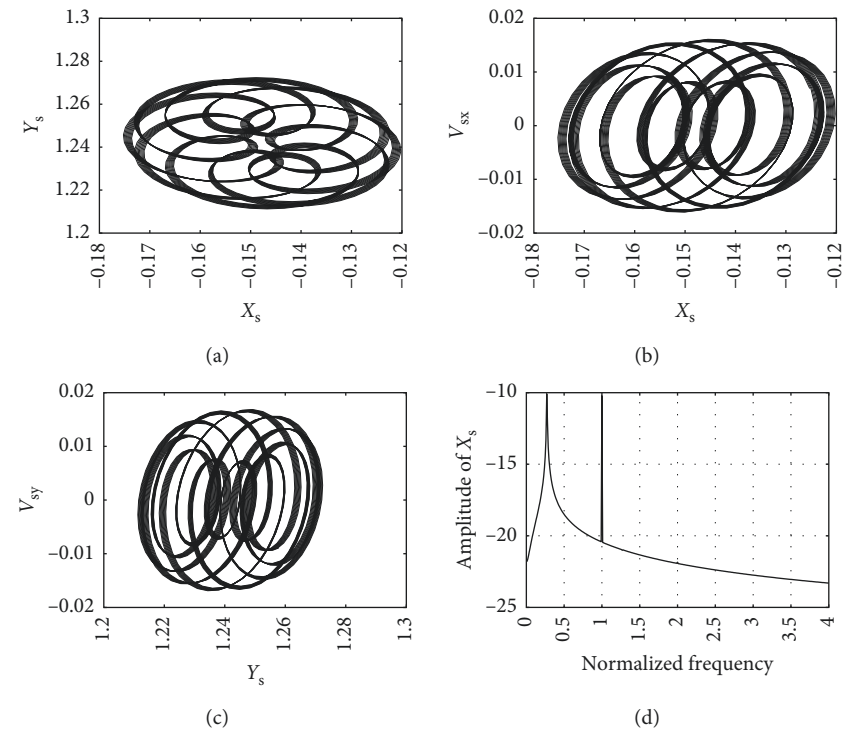

Figure 8: Continued.

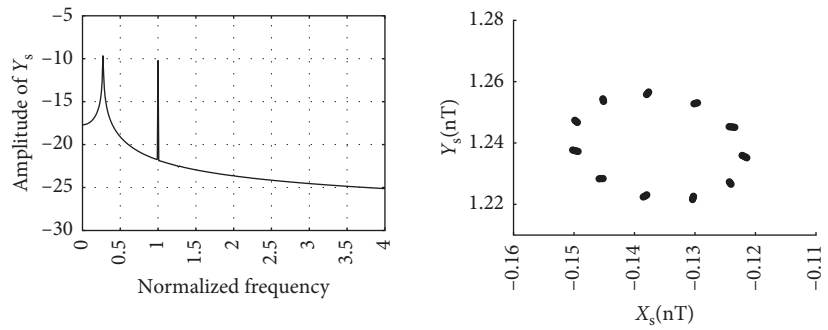

Figure 8: Obits, Poincare map, and amplitude spectrum of rotor center (m_s = 1 kg, ξ = 0.005, k = 4e6N/m, A = 1μm, and N = 5).

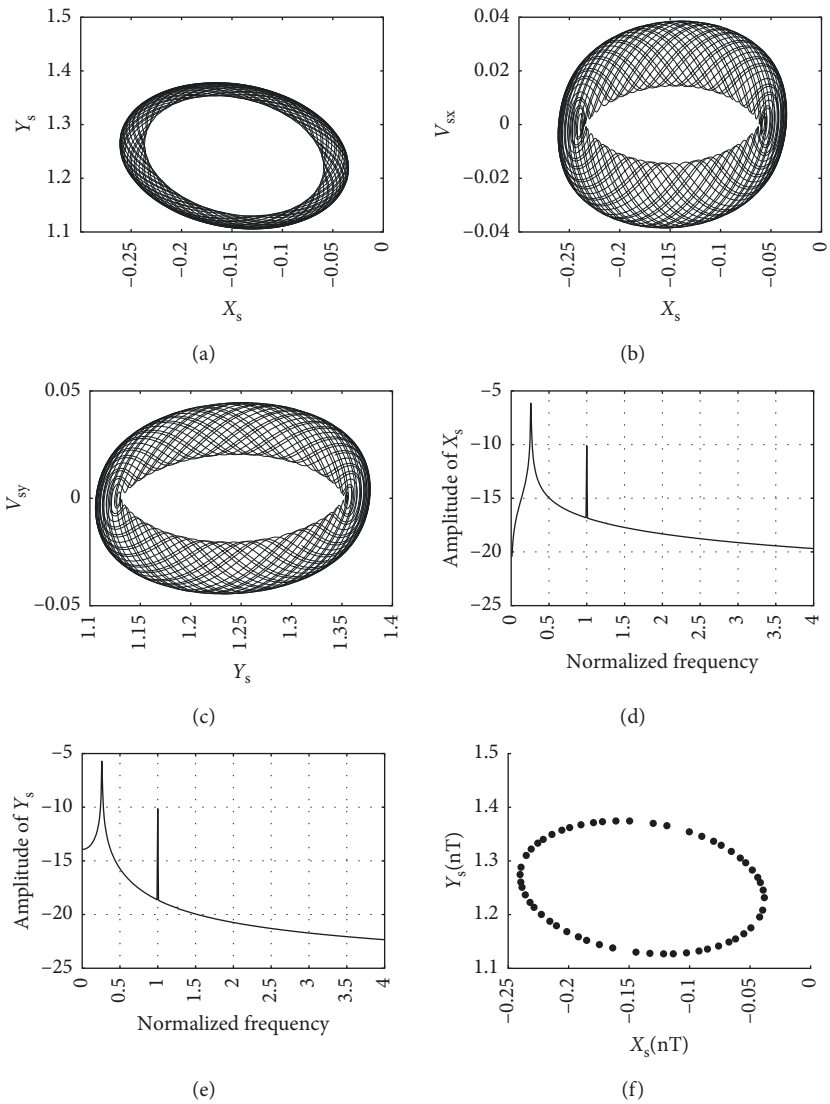

Figure 9: Obits, Poincare map, and amplitude spectrum of rotor center (m_s = 1.1 kg, ξ = 0.005, k = 4e6N/m, A = 1μm, and N = 5).

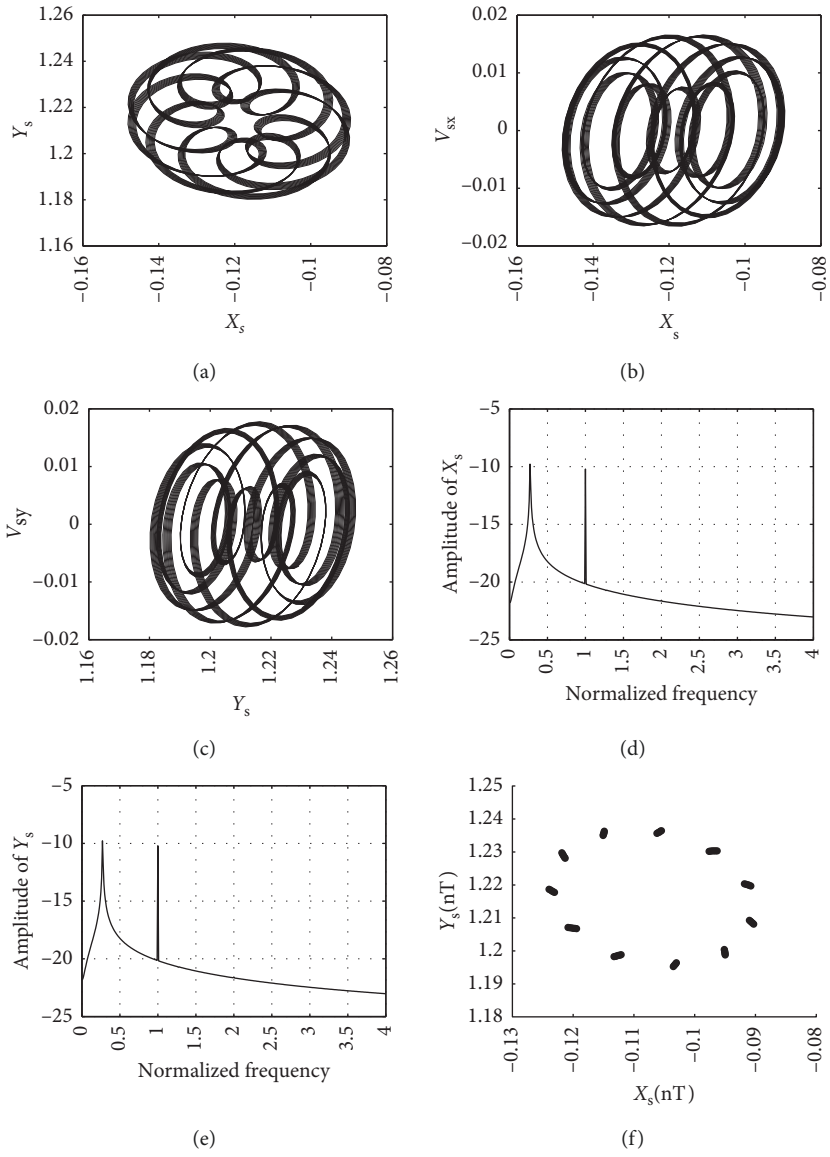

Figure 10: Obits, Poincare map, and amplitude spectrum of rotor center (m_s = 1 kg, ξ = 0.005, k = 4e6N/m, A = 1μm, and N = 3).

Figure 14 displays the bifurcation maps of the surface waviness in the axial direction. In this solution, m_s = 1 kg, ξ = 0.005, k = 4e6N/m, and A = 1μm are used. By comparing with the flat surface bearing system, we can conclude that the nonlinear dynamic performance of the system with axial surface waviness is similar to that of the system with flat surface. The discrete point of the system with axial surface waviness is 0.2 kg, a little bigger than that of the system with flat surface (0.19 kg). But the existence of surface waviness results in the decrease of the minimum gas film which easily causes the collision friction between rotor and bearing.

5. Conclusions

In this paper, the effects of surface waviness in circumferential and axial direction to the nonlinear dynamic characteristics of the rotor-bearing system with elastomer suspension have been investigated. The nonlinear dynamic behaviors under different conditions have been investigated by inspecting the rotor center obits, logarithm spectrum maps, and Poincare maps. The results of this study are more applied to the practical engineering and can provide a forward guidance of the manufacture for the bearing.

By comparing with the rotor-bearing system with flat surface, the surface waviness in circumferential direction does raise the stability of the system. For rotor-bearings system with surface waviness in circumferential direction (N = 5 and A = 1μm), the discrete point in the bifurcation diagram (0.75 kg) is much bigger than that of flat surface system (0.18 kg).

Three values (N = 3, 5, and 7) of the number of surface waviness are investigated and compared. The nonlinear dynamic performance is insensitive to the number of the waviness in circumferential direction. With the increase of the number of the waviness, the amplitude of the vibration declines slightly.

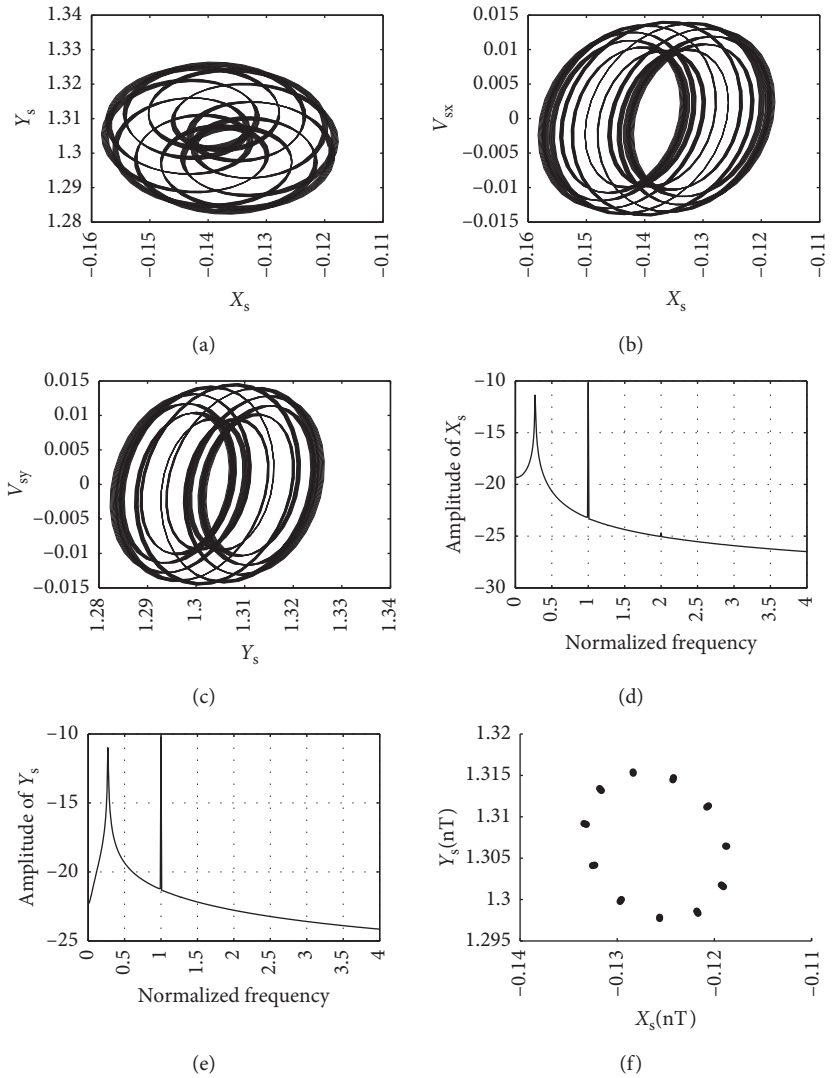

Figure 11: Obits, Poincare map, and amplitude spectrum of rotor center (m_s = 1 kg, ξ = 0.005, k = 4e6N/m, A = 1μm, and N = 7).

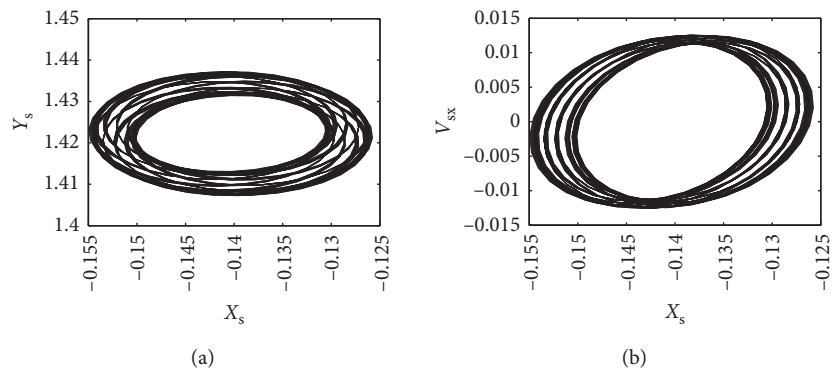

Figure 12: Continued.

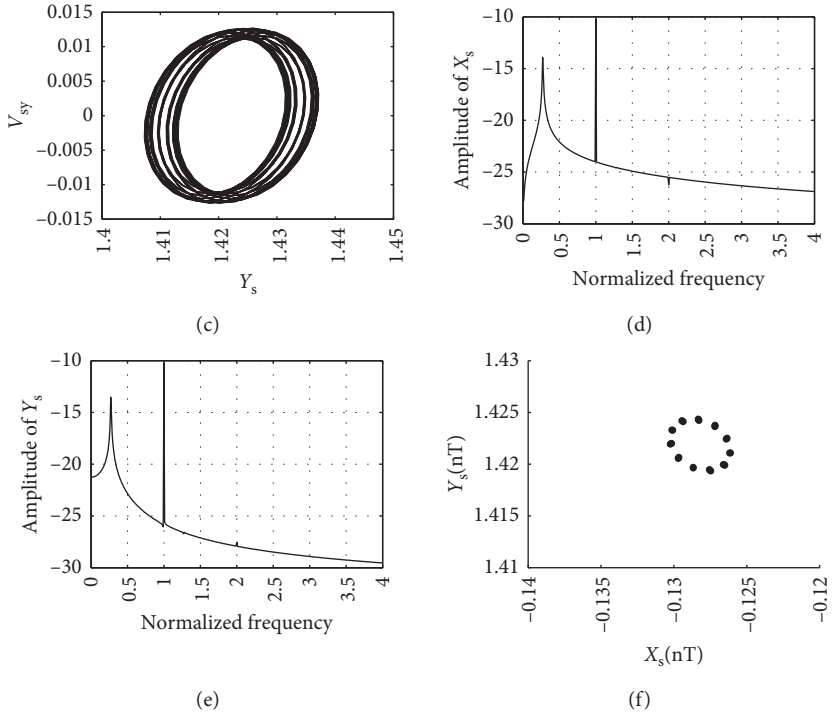

Figure 12: Obits, Poincare map, and amplitude spectrum of rotor center (m_s = 1 kg, ξ = 0.005, k = 4e6N/m, A = 2μm, and N = 5).

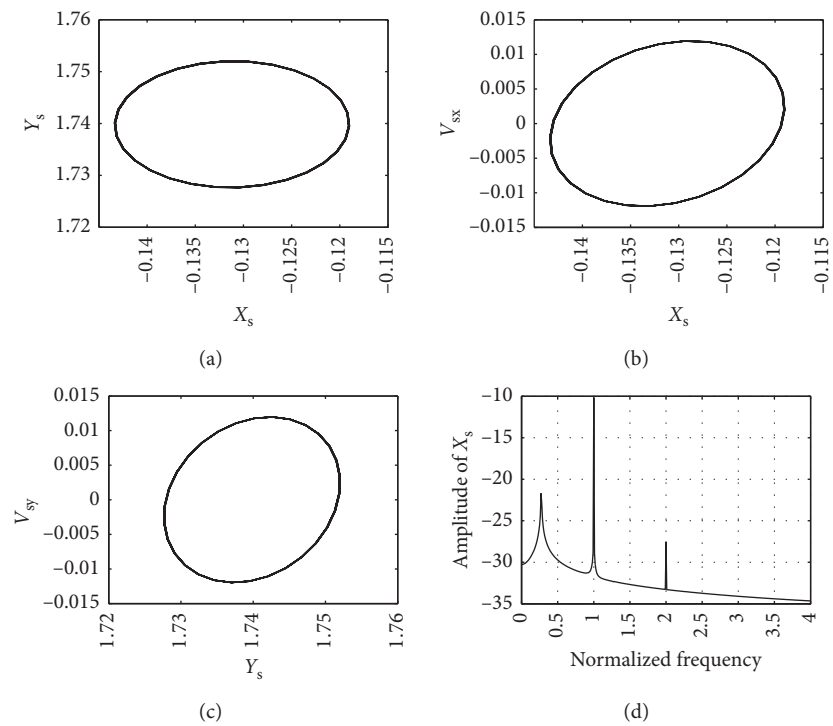

Figure 13: Continued.

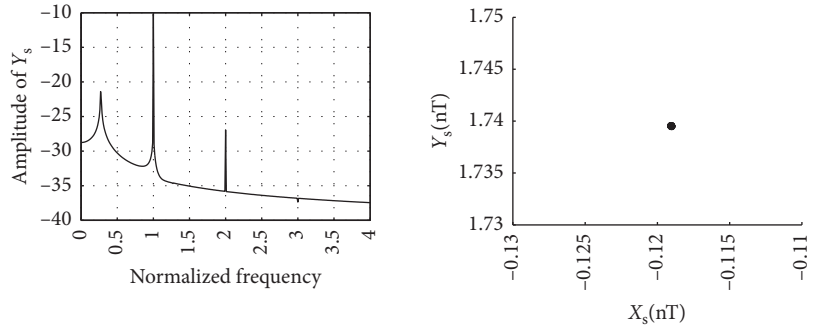

(e) (f)

Figure 13: Obits, Poincare map, and amplitude spectrum of rotor center (m_s =1 kg, ξ = 0.005, k = 4e6N/m, A = 3μm, and N = 5).

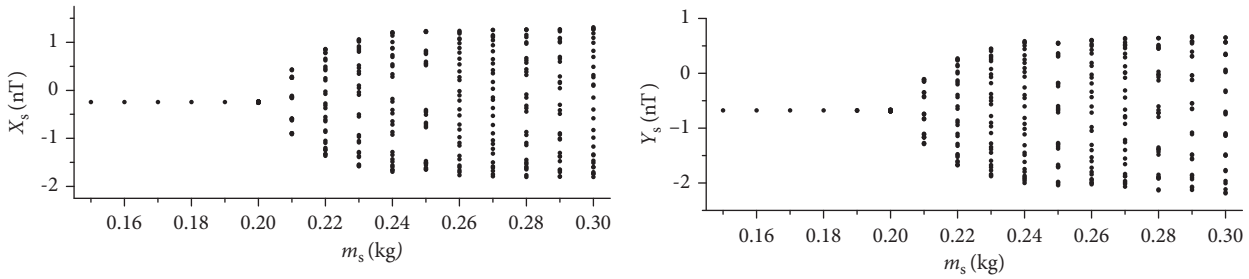

(a) (b)

Figure 14: Bifurcation diagrams of rotor center with axial surface waviness: (a) X_s (nT) and (b) Y_s (nT) versus half mass of rotor.

The increase of the amplitude of the surface waviness in circumferential can improve the static and dynamic performance of the bearing obviously. With the increase of the amplitude, the motion of the system is changed from quasiperiodic motion to regular periodic motion. Thus, the large amplitude can increase the stability of the system.

The effect of waviness in the axial direction is investigated by comparing with the flat surface. The axial surface waviness cannot change the nonlinear dynamic performance of the system. But the existence of the waviness can reduce the minimum gas clearance which is damage for the bearing.

Nomenclatures

A: Amplitude of the waves on the surface, m
A_{sx}, A_{sy}: Dimensionless horizontal and vertical acceleration of rotor
A_{bx}, A_{by}: Dimensionless horizontal and vertical acceleration of bearing
Cr: Average gas film clearance, m
d: Diameter of the rotor, m
e_{ub}: Mass eccentricity of the rotor, m
f_{gx}, f_{gy}: Supporting forces in horizontal and vertical directions, N
f_{ex}, f_{ey}: External forces in horizontal and vertical directions, N
f_d: Damping force of elastomer, N
F_{gx}, F_{gy}: Dimensionless supporting forces in horizontal and vertical directions
F: Defined as $\sqrt{F_{gx}^2 + F_{gy}^2}$
φ: Defined as $\tan^{-1}(F_{gx}/F_{gy})$
F_{ex}, F_{ey}: Dimensionless external forces in horizontal and vertical directions
H: Dimensionless film thickness between shaft and bearing
h: Film thickness, m
k, c: Stiffness (N/m) and damping $(N \cdot s/m)$ of elastic damper
γ: Damping exponent
K, C: Dimensionless stiffness and damping of damper
ξ: Dimensionless damping coefficient of elastomer, $\xi = c/2\sqrt{km_b}$
L: Length of journal bearing, m
m_s: One-half mass of rotor, Kg
m_b: Mass of bearing, Kg
M_s, M_b: Dimensionless mass of rotor and bearing
N: Number of waviness
p: Pressure, N/m^2
P: Dimensionless pressure
P_a: Atmosphere pressure, N/m^2
R: Radius of shaft, m
t: Time, s
τ: Dimensionless time, $\bar{\omega}t$
U: Peripheral speed of rotor in dynamical state, m/s
μ: Fluid kinematic viscosity, $Pa \cdot s$

V_{sx}, V_{sy}: Dimensionless horizontal and vertical velocity of rotor
V_{bx}, V_{by}: Dimensionless horizontal and vertical velocity of bearing
ϖ: Angular speed of rotor, rad/s
x, y: Horizontal and vertical coordinates, m
X_s, Y_s: Dimensionless horizontal and vertical displacement of rotor
X_b, Y_b: Dimensionless horizontal and vertical displacement of bearing
X_j, Y_j: Dimensionless displacement of rotor relative to the bearing in horizontal and vertical directions ($X_j = X_s - X_b; Y_j = Y_s - Y_b$)
Λ: Bearing number
ε: Eccentricity ratio of the system
δ: Height distribution of waviness, m
λ: Wavelength of surface waviness, m
θ, η: Dimensionless coordinate in circumferential and axial directions
n: Time level
i, j: Grid location in circumferential and axial directions
b: Parameters of bearing
s: Parameters of rotor
0: Initial parameter.

Data Availability

The data used to support the findings of this study have been deposited in the figshare repository (DOI: 10.6084/m9.figshare.6449477).

Conflicts of Interest

The authors declare that they have no conflicts of interest.

Acknowledgments

This work was supported by the fund from the National Research and Development Project for Key Scientific Instruments (ZDYZ2014-1) and the fund from the State Key Laboratory of Technologies in Space Cryogenic Propellants (SKLTSCP1604).

References

[1] R. Rashidi, A. Karami Mohammadi, and F. Bakhtiari Nejad, "Bifurcation and nonlinear dynamic analysis of a rigid rotor supported by two-lobe noncircular gas-lubricated journal bearing system," *Nonlinear Dynamics*, vol. 61, no. 4, pp. 783–802, 2010.

[2] R. Rashidi, A. Karami Mohammadi, and F. Bakhtiari Nejad, "Preload effect on nonlinear dynamic behavior of a rigid rotor supported by noncircular gas-lubricated journal bearing systems," *Nonlinear Dynamics*, vol. 60, no. 3, pp. 231–253, 2010.

[3] H. E. Rasheed, "Effect of surface waviness on the hydrodynamic lubrication of a plain cylindrical sliding element bearing," *Wear*, vol. 223, no. 1–2, pp. 1–6, 1998.

[4] F. Dimofte, "Wave journal bearing with compressible lubricant—part I: the wave bearing concept and a comparison to the plain circular bearing," *Tribology Transactions*, vol. 38, no. 1, pp. 153–160, 1995.

[5] F. Dimofte, "Wave journal bearing with compressible lubricant—part II: a comparison of the wave bearing with a wave-groove bearing and a lobe bearing," *Tribology Transactions*, vol. 38, no. 2, pp. 364–372, 1995.

[6] Y. B. P. Kwan and J. B. Post, "A tolerancing procedure for inherently compensated, rectangular aerostatic thrust bearings," *Tribology International*, vol. 33, no. 8, pp. 581–585, 2000.

[7] T. Nagaraju, S. C. Sharma, and S. C. Jain, "Study of orifice compensated hole-entry hybrid journal bearing considering surface roughness and flexibility effects," *Tribology International*, vol. 39, no. 7, pp. 715–725, 2006.

[8] N. M. Ene, F. Dimofte, and T. G. Keith Jr., "A stability analysis for a hydrodynamic three-wave journal bearing," *Tribology International*, vol. 41, no. 5, pp. 434–442, 2007.

[9] S. C. Sharma and P. B. Kushare, "Two lobe non-recessed roughened hybrid journal bearing – a comparative study," *Tribology International*, vol. 83, pp. 51–68, 2015.

[10] X. Wang, Q. Xu, B. Wang, L. Zhang, H. Yang, and Z. Peng, "Effect of surface waviness on the static performance of aerostatic journal bearings," *Tribology International*, vol. 103, pp. 394–405, 2016.

[11] W. A. Gross and E. C. Zachmanaglou, "Perturbation solutions for gas-lubricating films," *Journal of Basic Engineering*, vol. 83, no. 2, pp. 139–144, 1961.

[12] G. Belforte, T. Raparelli, and V. Viktorov, "Modeling and identification of gas journal bearings: self-acting gas bearing results," *Yale Journal of Biology*, vol. 124, no. 4, pp. 441–445, 2002.

[13] L. Yang, S. Qi, and L. Yu, "Numerical analysis on dynamic coefficients of self-acting gas-lubricated tilting-pad journal bearings," *Journal of Tribology*, vol. 130, no. 1, pp. 125–128, 2008.

[14] P. Yu, X. Chen, X. Wang, and W. Jiang, "Frequency-dependent nonlinear dynamic stiffness of aerostatic bearings subjected to external perturbations," *International Journal of Precision Engineering and Manufacturing*, vol. 16, no. 8, pp. 1771–1777, 2015.

[15] Y. B. Kim and S. T. Noah, "Bifurcation analysis for a modified Jeffcott rotor with bearing clearances," *Nonlinear Dynamics*, vol. 1, no. 3, pp. 221–241, 1990.

[16] C. Wang and H. Yau, "Theoretical analysis of high speed spindle air bearings by a hybrid numerical method," *Applied Mathematics and Computation*, vol. 217, no. 5, pp. 2084–2096, 2010.

[17] C. Wang, "Theoretical and nonlinear behavior analysis of a flexible rotor supported by a relative short herringbone-grooved gas journal-bearing system," *Physica D: Nonlinear Phenomena*, vol. 237, no. 18, pp. 2282–2295, 2008.

[18] C. Wang, M. Jang, and Y. Yeh, "Bifurcation and nonlinear dynamic analysis of a flexible rotor supported by relative short gas journal bearings," *Chaos, Solitons and Fractals*, vol. 32, no. 2, pp. 566–582, 2007.

[19] J. Wang and C. Wang, "Nonlinear dynamic and bifurcation analysis of short aerodynamic journal bearings," *Tribology International*, vol. 38, no. 8, pp. 740–748, 2005.

[20] C. Wang and C. Chen, "Bifurcation analysis of self-acting gas journal bearings," *Journal of Tribology*, vol. 123, no. 4, pp. 755–767, 2001.

[21] M. A. Hassini and M. Arghir, "A simplified nonlinear transient analysis method for gas bearings," *Journal of Tribology*, vol. 134, no. 1, article 11704, 2012.
[22] A. Abbasi, S. E. Khadem, S. Bab, and M. I. Friswell, "Vibration control of a rotor supported by journal bearings and an asymmetric high-static low-dynamic stiffness suspension," *Nonlinear Dynamics*, vol. 85, no. 1, pp. 525–545, 2016.
[23] P. Yang, K. Zhu, and X. Wang, "On the non-linear stability of self-acting gas journal bearings," *Tribology International*, vol. 42, no. 1, pp. 71–76, 2009.
[24] X. Wang, Q. Xu, M. Huang, L. Zhang, and Z. Peng, "Effects of journal rotation and surface waviness on the dynamic performance of aerostatic journal bearings," *Tribology International*, vol. 112, pp. 1–9, 2017.
[25] S. Yan, E. H. Dowell, and B. Lin, "Effects of nonlinear damping suspension on nonperiodic motions of a flexible rotor in journal bearings," *Nonlinear Dynamics*, vol. 78, no. 2, pp. 1435–1450, 2014.
[26] G. Zhang, Y. Sun, Z. Liu, M. Zhang, and J. Yan, "Dynamic characteristics of self-acting gas bearing–flexible rotor coupling system based on the forecasting orbit method," *Nonlinear Dynamics*, vol. 69, no. 1, pp. 341–355, 2012.
[27] F. Rüdinger, "Optimal vibration absorber with nonlinear viscous power law damping and white noise excitation," *Journal of Engineering Mechanics*, vol. 132, no. 1, pp. 46–53, 2006.
[28] R. D. Brown, P. Addison, and A. Chan, "Chaos in the unbalance response of journal bearings," *Nonlinear Dynamics*, vol. 5, no. 4, pp. 421–432, 1994.
[29] G. Adiletta, A. R. Guido, and C. Rossi, "Chaotic motions of a rigid rotor in short journal bearings," *Nonlinear Dynamics*, vol. 10, no. 3, pp. 251–269, 1996.